A&A 387, 624–634 (2002)
DOI: 10.1051/0004-6361:20020354

Astronomy & Astrophysics

VLT/UVES and WHT/UES absorption spectroscopy of the circumstellar envelope of IRC +10° 216 using background stars⋆

First results and a search for DIBs

T. R. Kendall[1], N. Mauron[2], J. McCombie[3], and P. J. Sarre[3]

[1] Centro de Astronomia e Astrofísica da Universidade de Lisboa, Observatório Astronómico de Lisboa, Tapada da Ajuda, 1349-018 Lisboa, Portugal
[2] Groupe d'Astrophysique, CNRS and Université de Montpellier, Case 072, Place Bataillon, 34095 Montpellier Cedex 05, France
e-mail: mauron@graal.univ-montp2.fr
[3] School of Chemistry, The University of Nottingham, University Park, Nottingham, NG7 2RD, UK
e-mail: June.McCombie@nottingham.ac.uk; Peter.Sarre@nottingham.ac.uk⋆

Received 7 January 2002 / Accepted 7 March 2002

Abstract. A unique and novel set of observations has been undertaken to probe the circumstellar envelope (CSE) of the nearby (130 pc) carbon star IRC +10° 216 using optical absorption spectroscopy towards *background stars* lying beyond the envelope. The primary aim of the observations is to search for diffuse band (DIB) carriers in the CSE, for which the mass-losing envelopes of carbon stars are a likely place of origin. Our principal target is a $V = 16$ G-type star located 37″ from IRC +10° 216 and was observed with VLT/UVES. A detailed model atmosphere and abundance analysis shows that it is somewhat metal-poor and has confirmed that it lies far beyond IRC +10° 216. The *circumstellar* H+2H$_2$ column density expected along the line of sight towards this target is relatively high, $\sim 2 \times 10^{21}$ cm^{-2}, and is large compared to that derived from the small *interstellar* extinction estimated in the zone of IRC +10° 216 at $b = +43°$, $E_{B-V} < 0.03$ mag. The CSE is certainly detected in the K I resonance lines, which are centred at the heliocentric velocity of IRC +10° 216 and have $FWHM \sim 30$ km s^{-1}, consistent with twice the terminal expansion velocity of the circumstellar gas. The data show also that circumstellar Na I is very probably detected, as seen towards two background stars. The strongest DIB (6284 Å) present in the UVES wavelength coverage is detected but very probably arises in the foreground ISM. No DIB is detected at 6614 Å, or elsewhere. Overall, the data suggest that the DIB carriers, if present in the CSE, have a low abundance relative to H in the C-rich envelope of IRC +10° 216, in comparison with this ratio in the ISM.

Key words. stars: individual: IRC +10° 216 – stars: carbon – stars: circumstellar matter – ISM: lines and bands – ISM: molecules

1. Introduction

Diffuse interstellar bands (DIBs) have been observed in the visible spectra of reddened OB stars for over seventy years; over 200 are now known, but the identification of the DIB carrier(s) remains a major challenge in molecular astrophysics (Herbig 1995). Many diverse origins have been advanced, such as carbon chains (Douglas 1977; Thaddeus et al. 1993), polycyclic aromatic hydrocarbons (PAHs) (Léger et al. 1987; Salama et al. 1996), fullerenes (Kroto & Jura 1992; Foing & Ehrenfreud 1997) or even H_2 (Sorokin & Glownia 1996; Ubachs et al. 1997), among many others. None has been confirmed with certainty. In addition to the intrinsic importance of identification of this ubiquitous material, DIB carriers may provide crucial information on the nature of interstellar matter, including dust composition and extinction properties, gas-phase and dust based chemistry and physics and, conceivably, astrobiology (Herbig 1995; Williams 1996; Miles & Sarre 1993).

A key issue is to discover where DIB carriers are formed, and there are several reasons to consider the dense outflows of asymptotic giant branch (AGB) carbon stars as a likely source. First, these stars inject into the ISM

Send offprint requests to: T. R. Kendall,
e-mail: tkendall@oal.ul.pt

⋆ Based on observations made with the ESO VLT 8 m telescope with UVES (program 66.C-0220), WHT/UES (La Palma) and the 1.2 m telescope of the Haute–Provence Observatory, France.

a large amount of carbon-rich material. Carbon chains (polyynes, C_3, C_5), to which the DIB carriers may be related, are known to be present in the circumstellar envelope (CSE) of IRC +10° 216, the nearest dusty, molecule-rich carbon star with a high mass-loss rate. PAH molecules or fullerenes may also be present. A further strong argument is the fact that DIBs have been detected (in emission) in the circumstellar matter of two carbon-rich objects; The Red Rectangle (HD 44179, Sarre et al. 1995), which is believed to be in a post-AGB evolutionary phase, and the H-deficient R CrB star V854 Cen at minimum light (Rao & Lambert 1993).

The first search for diffuse bands in absorption in a circumstellar envelope was attempted by Snow & Wallerstein (1972) and Snow (1973), and no such signature was found. A more detailed search for diffuse band absorption in carbon-rich CSE was performed by Le Bertre (1990), and extended by Le Bertre & Lequeux (1992, 1993). In the majority of cases, these authors did not find evidence of diffuse circumstellar bands, and concluded that the band carriers should be, in general, depleted in carbon-rich circumstellar matter (with the exception of a very few objects such as CS 776, which we reconsider in Sect. 6). Nor did they find more intense diffuse bands in sources with strong unidentified infrared bands (UIBs), such as NGC 7027. However, they proposed that nitrogen may be an important constituent of the carriers, or play a role in their formation. Spectra recorded towards the central star of IRC + 10° 216 revealed the presence of circumstellar C_2, but no diffuse band absorptions were reported (Bakker et al. 1997).

More recently, effort has been concentrated on carbon-rich proto-planetary nebulae with F– or G–type spectra (Zacs et al. 1999; Klochkova et al. 1999), demonstrating that diffuse band absorptions can be observed toward targets of later spectral type with more crowded stellar spectra, than the reddened OB stars typically used for ISM studies of this nature. Zacs et al. (1999) have observed a feature on the red wing of the λ5780 DIB, seen towards the G–type post-AGB object HD 178921, which they claim may arise in the CSE. They also propose possible circumstellar diffuse band absorptions at $\lambda\lambda$5780, 6597 and 6196 towards another G–type evolved object, SAO 34504 (IRAS 22272+5435). Finally, Klochkova et al. (2000b) (see also Klochkova et al. 1999; Klochkova et al. 2000a) proposed a circumstellar origin for diffuse band features in the spectra of IRAS 23304+6147, IRAS 04296+3429, IRAS 22223+4327 and the Egg Nebula, via velocity arguments.

In this study, we report the first results of a search for DIBs directly in the CSE of IRC +10° 216, by observing background stars seen through the envelope. Section 2 describes the targets that were selected and their characteristics. The observations, which were made with the ESO VLT/UVES and the La Palma WHT/UES spectrographs, are described in Sect. 3. A model atmosphere analysis of our principal target has been performed, and the results are given in Sect. 4 together with details in the Appendix. Our main results on circumstellar K I, Na I, and our search for DIBs are presented in Sect. 5, and their implications are discussed in Sect. 6. We conclude in Sect. 7 with a summary of our findings.

2. Target background stars in the field of IRC +10° 216

Deep images of IRC +10° 216 in the B and V passbands, obtained by Mauron & Huggins (1999), have revealed its CSE as seen in dust-scattered, ambient galactic light. The envelope is structured in thin circular incomplete shells and extends out to ∼3′, which corresponds roughly to the CO extension (Huggins 1995). Within 15″ of the centre, IRC +10° 216 is opaque, but from roughly 15″ to 200″, it is possible to see through the CSE at optical wavelengths. Potential background targets are galactic field stars or very faint $V = 20-24$ mag galaxies (see Fig. 1). Based on UBV photometry of the field obtained with the CCD camera of the 1.2 m telescope of Haute–Provence Observatory (to be reported in Mauron et al. 2002), a first selection of targets was performed. Provided it can be shown that such targets are located behind the CSE, obvious candidates are those stars being angularly the nearest to IRC +10° 216 (to maximize circumstellar column density), the brightest in apparent magnitude (to permit high signal-to-noise ratio, high resolution spectroscopy) and the bluest in colour index (to minimize confusion by photospheric features in the spectrum).

Table 1 lists the targets studied in this paper, together with photometric data and our estimates of distances which are discussed below. The targets are identified in Fig. 1. The relevant circumstellar quantities are also listed in Table 1. The impact parameter r and tangential (line of sight) circumstellar column densities of hydrogen are derived using the following values for IRC +10° 216: $v_{\rm outflow} = 15$ km s^{-1}, $d = 130$ pc and $\dot{M}_{\rm H} = 2 \times 10^{-5}\, M_\odot$ yr^{-1} (Glassgold 1996; Groenewegen et al. 1998).

The uncertainty in the $N_{\rm H}$ (exactly N(H+2H$_2$)) values demands examination. First, there is some uncertainty in $\dot{M}_{\rm H}$ and d; however, it can be remarked that $N_{\rm H}$ scales as $\dot{M}_{\rm H}/d$, and this ratio does not change by more than 30% between the case $d = 110$ pc and $d = 190$ pc (from Tables 2 and 6 of Groenewegen et al. 1998), because it is well constrained by observations. A more serious uncertainty is due to the fact that the CSE is inhomogeneous (clumpy). More precisely, the envelope density distribution observed from optical images is obviously not consistent with the smooth r^{-2} law assumed for these $N_{\rm H}$ estimates. Hence the listed values of $N_{\rm H}$ are perhaps incorrect by as much as a factor of 2 in both directions, i.e., the true $N_{\rm H}$ may be *higher or lower* than these estimates. We note, however, that the mass loss rate measured at offsets $\Theta > 50''$ is found to be a factor of 5 larger than the one adopted above, as found from many observations probing, in general, layers nearer to the

Table 1. Parameters for the observed stars and circumstellar quantities. The distances d are best estimates derived from our photometric and spectroscopic data (see Sect. 4); the angle Θ ($''$) is the angular offset from IRC +10° 216; $N_{\rm H}^{\rm tang}$ is the expected line-of-sight circumstellar column density; $A_{\rm v}$ is the *circumstellar* extinction derived from $N_{\rm H}^{\rm tang}$ when *assuming* a $N_{\rm H}/A_{\rm v}$ ratio typical of diffuse interstellar matter (see Sect. 2).

USNO 0975-0633-	name	V	$B-V$	Spec.	d/pc	$\Theta/''$	r/cm	$N_{\rm H}^{\rm tang}/{\rm cm}^{-2}$	$A_{\rm v}$/mag
6975	Star 6	16.00	0.78	G2:	∼1400	37	6.8×10^{16}	1.8×10^{21}	0.9
6812	Star C	12.4	-	F8:	∼500	153	3.0×10^{17}	4.1×10^{20}	0.2

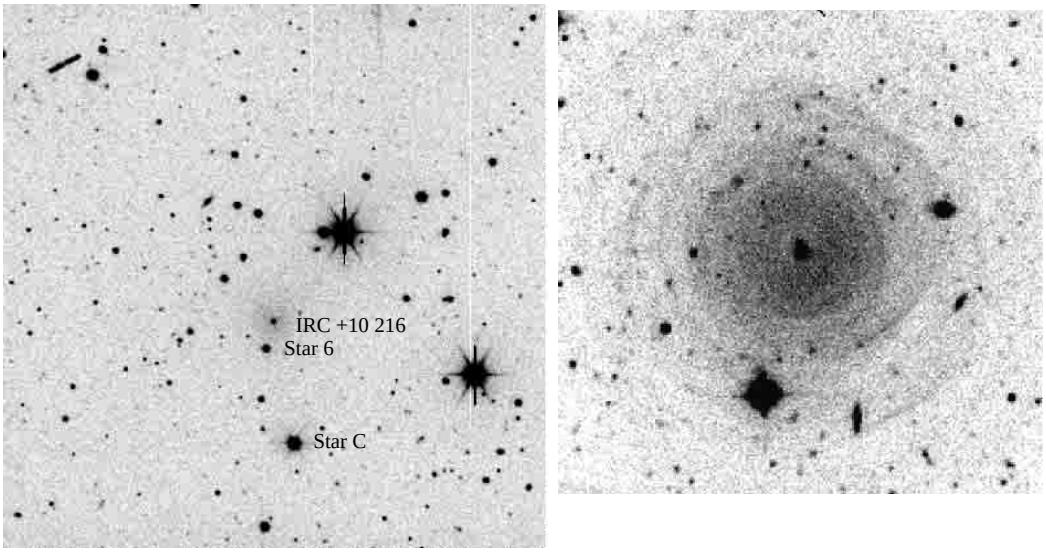

Fig. 1. *Left panel*: the $12.4\times12.4'$ field around IRC +10° 216, imaged in the V-band at the 1.2 m Haute–Provence telescope. Stars 6 and C are labelled. *Right panel*: deep $2\times2'$ B-band CFHT image showing the IRC +10° 216 envelope in dust scattered ambient galactic light. Star 6 is the bright star located 37$''$ below and slightly to the left of IRC +10° 216.

centre (Groenewegen et al. 1998). Consequently, our $N_{\rm H}$ values could in fact be *underestimates* of the true hydrogen column densities. We have also listed in Table 1, for illustration, the corresponding $A_{\rm v}$ values *if one adopts* the relation for the diffuse ISM, $N_{\rm H}/A_{\rm v} = 2.1\times10^{21}$ cm^{-2} mag^{-1} (Bohlin et al. 1978), but we note the actual circumstellar dust absorption could be lower (Omont 1991).

Concerning the distance of Star 6, examination of its $B-V$ and $U-B$ colour indices (0.78 and 0.31 respectively), faintness and high galactic latitude ($b = +43°$) suggests that it may be a G–type (or reddened F) dwarf, or perhaps a metal-poor subdwarf. It is too blue to be a nearby M dwarf which would have $B-V \sim 1.5$. Estimating a distance relies on the adopted absolute magnitude and estimation of the interstellar and/or circumstellar absorption and reddening. Because of the high galactic latitude, the interstellar extinction is very low, and the maps of Burnstein & Heiles (1982) suggest $A_{\rm v} < 0.1$ mag. in a large zone around IRC +10° 216. For Star 6 at least, the circumstellar column density should be larger than the interstellar one if our estimate of circumstellar column density above is correct. Making various assumptions concerning the amount of circumstellar dust extinction and reddening law (which is uncertain), and adopting subdwarf luminosities, e.g. $M_{\rm v} = +6.8$ (Allen 1973), we obtain for Star 6 a distance between 430 and 1100 pc, i.e. substantially greater than the distance to IRC +10° 216. Larger distances would be inferred if one assumes a solar-like dwarf type, or a giant type.

No UBV data could be obtained for Star C because of saturation. The USNOC catalogue provides $R = 13.0$ and $B-R = 0.2$, which is relatively blue and suggests, with considerable uncertainty, an A3 spectral type. If this is the case, with $V \sim 13$, and $M_{\rm v} \sim +1.7$, one derives a distance of 2100 pc. If however, the USNOC colour is in error by 0.5 mag, which is not unlikely, then the star is nearer a F2–type with $B-R = 0.7$, then again with $V \sim 13$ and now $M_{\rm v} \sim +3.6$, its distance is about 800 pc. Only if this star were as late as a K7V, with $B-R = 2.15$ (which is unlikely) and $M_{\rm v} \sim +7.3$, would its distance be ∼140 pc.

In conclusion, the two targets seem to lie at favourable distances beyond IRC +10° 216, i.e. beyond ∼130 pc. Unfortunately, neither Star C or 6 is present in the Hipparcos catalogue, preventing distance estimates using accurate parallaxes. However, the distances we estimate from photometry are very well confirmed by the spectral analysis described below. We note also that the expected circumstellar H column density for Star 6 would correspond to $A_{\rm v} = 0.9$ mag in the ISM: this is comparable to that towards stars with intervening diffuse clouds in the spectra of which DIBs are readily detected, as evidenced by studies of DIBs in lines of sight which intersect only a

single intervening diffuse cloud, with resultant low reddening (Cami et al. 1997; Weselak et al. 2000; Galazutdinov et al. 1998; Galazutdinov et al. 2000).

3. Observations and data reduction

3.1. WHT/UES observations

Stars 6 and C were observed with the William Herschel Telescope (WHT) at La Palma, Canary Islands on the nights February 10 and 11, 2000, using the Utrecht Echelle spectrograph (UES). With a slit width of 1.1″, the 31 mm^{-1} grating and the SiTe1 2048×2048 24 μm pixel CCD as detector, the resultant wavelength coverage was ∼3820−7000 Å at $R \equiv \lambda/\Delta\lambda = 50\,000$. In spite of over 9 hours of on-star integration for Star 6, the signal-to-noise ratio nowhere exceeded 10, even in the peaks of the best orders. However, for Star C, a total integration time of 9000 s (in 1800 s exposures) yielded a peak S/N ratio of ∼60. A 120 s exposure spectrum of the star ν Leo with $V = 5.26$, $d = 55$ pc and lying 2.5° from IRC +10° 216, was also obtained with the same instrumental setup, in order to provide information on foreground interstellar absorption and as a comparison spectrum for telluric lines.

Data reduction was performed using standard IRAF[1] procedures within the ECHELLE package. After subtraction of the bias level, images were subsetted to avoid edge effects and flat-fielded using lamp flats taken at the beginning and end of each night. Spectra were then extracted using the DOECSLIT task, allowing cosmic ray removal, inter-order background subtraction, optimal spectrum extraction and wavelength calibration using Thorium-Argon arc exposures which bracketed each stellar exposure. After heliocentric correction, the spectra were co-added using the SCOMBINE task and output in ASCII format to the STARLINK package DIPSO (Howarth et al. 1998) for subsequent analysis.

3.2. VLT/UVES observations

Following the failure to obtain a spectrum of Star 6 at the WHT, ESO time on VLT/UT2 (Kueyen) with the Ultraviolet and Visual Echelle Spectrograph (UVES), in service mode, was obtained. A total of 6 hours of integration time was achieved on Star 6 in a number of runs during December 2000 and January 2001. Using a 0.8″ slit width and both red and blue dichroics, spectra were obtained over six wavelength ranges: 3045–3870 Å, 3758–4980 Å, 4785–5761 Å, 5838–6811 Å, 6707–8523 Å and 8662–10430 Å, at a resolution $R = 50\,000$. Over a wide range of wavelength from ∼3758 Å to ∼8522 Å, continuum counts were sufficient to yield a signal-to-noise ratio approaching, and over certain ranges exceeding, 50. Data reduction was provided by the ESO/UVES reduction pipeline, based on the ESO MIDAS package. Pipeline reduced, wavelength calibrated spectra were then corrected for the heliocentric velocity and converted into ASCII format for output to DIPSO for co-addition and analysis.

[1] IRAF is distributed by the National Optical Astronomy Observatories, which is operated by the Association of Universities for Research in Astronomy, Inc. (AURA) under cooperative agreement with the National Science Foundation.

4. Analysis of the photospheres of the target stars

Prior to searching for diffuse band, molecular and atomic absorptions in the spectrum of Star 6, it was necessary to fully characterise the photospheric component of the spectrum. We used the Kurucz ATLAS9 model atmosphere grids (Kurucz 1991) to perform a detailed abundance analysis and ultimately (for Star 6 only) spectral synthesis. For clarity of the text, the details on the derivation of the atmospheric parameters of Star 6 from the UVES data are given in the Appendix, and only the results are reported here.

Firstly, the heliocentric radial velocity for Star 6 was found to be $+52.4 \pm 0.6$ km s^{-1}. This implies that photospheric components of e.g. atomic resonance lines (Na I, K I) are shifted well away from any absorptions arising in the IRC +10° 216 CSE at $v_{\rm helio} = -19.3$ km s^{-1}.

Secondly, the best-fit parameters for Star 6 were found to be: $T_{\rm eff} = 5650$ K, $\log g = 4.3$ (cgs), $V_{\rm turb} = 1.3$ km s^{-1} and [Fe/H] = −0.4 dex, relative to solar. Abundances for other elements are given in the Appendix. These results confirm that Star 6 is a low metallicity object of spectral type G, perhaps somewhat cooler than the Sun, with a very similar surface gravity. The metallicity suggests that Star 6 is likely to be a member of the thick disk population. Most importantly, adopting a luminosity class V yields an absolute magnitude $M_{\rm v} = +5.3$ for Star 6 (Lang 1991), suggesting a distance of 1400 pc and confirming that Star 6 is indeed well beyond IRC +10° 216.

Photospheric parameters and a spectroscopic distance have also been derived for Star C, yielding $T_{\rm eff} \sim 6250$ K, $\log g \sim 4.8 \pm 0.2$, $V_{\rm turb} \sim 2.1$ km s^{-1} and [Fe/H] ∼ −0.4 dex relative to solar. The heliocentric velocity is near 0 km s^{-1}. If luminosity class V, Star C has spectral type near F8, and $M_{\rm v} = +4.0$ yields a distance of 480 pc. If Star C is a subdwarf rather than a solar-type dwarf, then its absolute magnitude is ∼1.3 mag fainter (Allen 1973), hence the distance would be reduced by a factor of 1.8 to 260 pc, still twice the accepted distance of IRC +10° 216.

5. Results

5.1. K I lines

The spectrum recorded towards Star 6 exhibits very strong K I absorption between −5 and −35 km s^{-1} that is well removed from lines arising in the photosphere itself at +52.4 km s^{-1} (see Fig. 2). The three vertical lines in the figure mark absorption components at −27.4, −20.4 and −9.5 km s^{-1} that are repeated in both of the K I profiles, and are centred on the heliocentric velocity of IRC +10° 216 (−19.3 km s^{-1}). Moreover, the *FWHM*

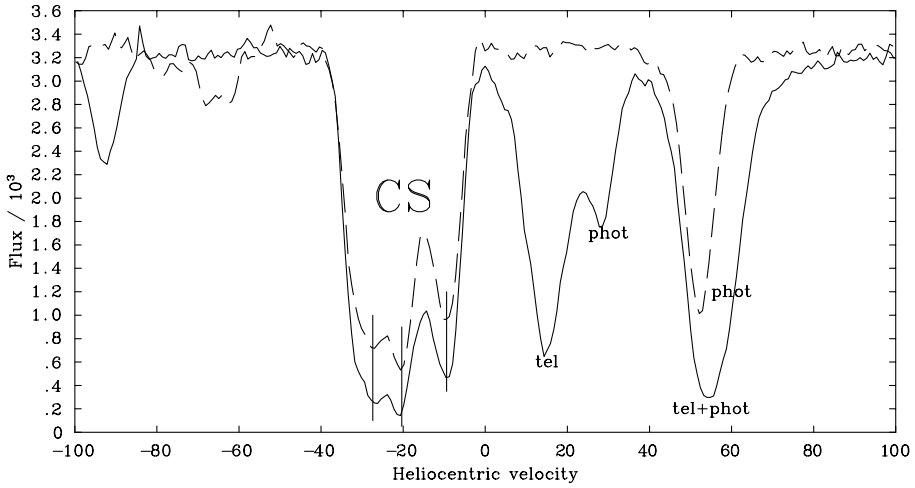

Fig. 2. K I lines in the VLT spectrum of Star 6, shown in heliocentric velocity space. The solid line is the K I 7665 Å profile, the dashed line K I 7699 Å. The three vertical lines trace circumstellar components in K I, centred very closely to the heliocentric velocity of IRC +10° 216 at −19.3 km s^{-1} .

of the overall K I profile, ∼28 km s^{-1}, is close to twice the known terminal expansion velocity of the gas in IRC +10° 216 CSE, and consistent with the known geometry of the line of sight through the CSE.

The equivalent widths of the 7665 and 7699 Å K I components are ∼630 and 525 mÅ respectively. Because of the low interstellar reddening in this region of the sky, $E_{B-V} \sim 0.03$, we can therefore exclude the possibility that these very strong K I lines are due to absorption by foreground or background diffuse interstellar matter. More precisely, for this low interstellar reddening, one would expect K I equivalent widths of the order of only 8 mÅ, within a factor of 2, based the survey of interstellar K I by Chaffee & White (1982).

Consequently, both the strengths and the velocity components of these K I lines provide clear evidence for an origin in the IRC +10° 216 circumstellar envelope.

Figure 3 shows the results of the spectral synthesis in the region of the two K I components, indicating that there is no significant contamination of the circumstellar signature by photospheric lines of any species. Furthermore, Fig. 4 shows the 7665 Å profile (lower panel) compared to a pure telluric spectrum (upper panel). Both spectra are uncorrected for the heliocentric velocity, i.e. they are both at the rest wavelength of telluric lines. The telluric spectrum is of a very metal-poor halo subdwarf F0 star, G64-12, obtained from the UVES archive, for which [Fe/H] = −3.03 (Axer et al. 1994). It can be seen that there is no telluric contamination of the circumstellar K I 7665 component.

5.2. Na I lines

Figure 5 shows the region of the Na D lines in the Star 6 spectrum recorded with VLT/UVES. As for K I, very strong absorption components are seen at velocities between −5 and −35 km s^{-1}, shifted away from the strong photospheric lines. Since these absorption components are saturated, there is little information in the profile shape, and no comparison has been performed between the profiles as was done for K I. The components are centred on the velocity of IRC +10° 216, and have a width commensurate with the gas expansion velocity, and it is likely that a large part of the absorption arises in the CSE of IRC +10° 216. However interstellar contamination cannot be ruled out: even at $E_{B-V} = 0.03$ some interstellar absorption may be expected. Although the spectral synthesis of the Na lines is poor, probably because NLTE effects are not taken into account, it shows that there is again no significant additional component arising from other species in the Star 6 photosphere.

Figure 6 shows spectra of Na I D lines from WHT/UES for comparison with the VLT K I and Na I Star 6 data. The signal-to-noise ratios of these spectra are ∼220 and ∼50 for ν Leo and Star C respectively. For Star C, the line profiles are very reminiscent of Star 6. Lying 153″ from IRC +10° 216, within the CO and dust envelope radii, it is likely that these spectra are also probing CS Na I in the IRC +10° 216 CSE. The heliocentric velocity is near 0 km s^{-1} (as measured using Hβ), so the profiles may be contaminated by photospheric Na I on the red wing. Unfortunately, the WHT spectra of Star C do not cover the K I resonance lines.

By contrast, the Na D lines in ν Leo are very weak (note the ordinate scale). With a spectral type of B9IV, there is no possibility of photospheric Na I in this object. The lines observed are interstellar in origin and are likely to be typical of the ISM in this direction, at least up to a distance of ∼60 pc. (ν Leo lies 2.5° from IRC+10°216).

5.3. Diffuse band absorptions

In diffuse ISM spectra, the strongest reasonably narrow DIBs lie at 5780 Å, 5797 Å, 6284 Å and 6614 Å. Owing to an instrumental gap in the data, the first two regions were not observed. However, the 6284 Å and 6614 Å regions have been closely examined. In Fig. 7, the region of the

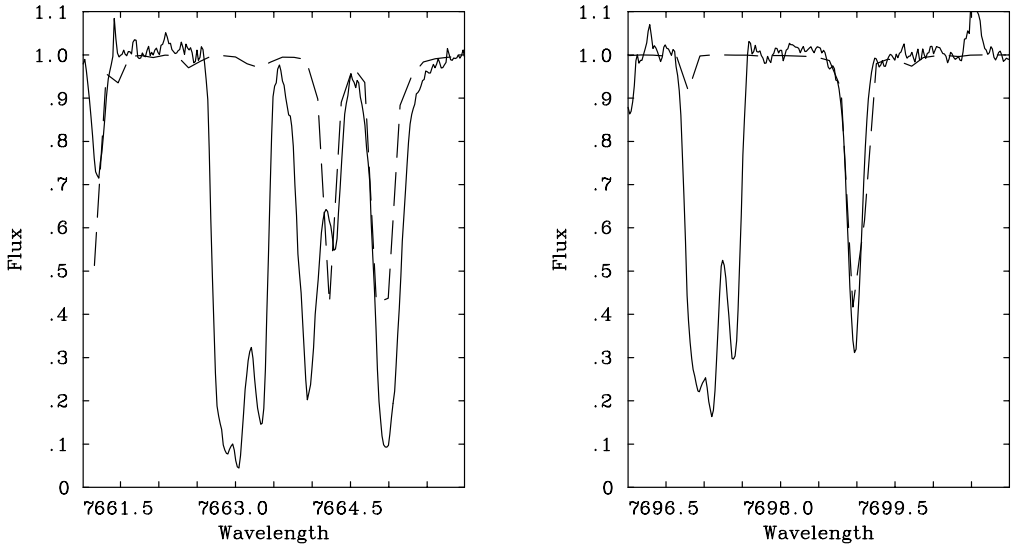

Fig. 3. K I lines in the VLT spectrum of Star 6, shown corrected for the stellar radial velocity. The dashed lines are a spectral synthesis (for details see text). The CS K I components are clearly unaffected by other photospheric lines.

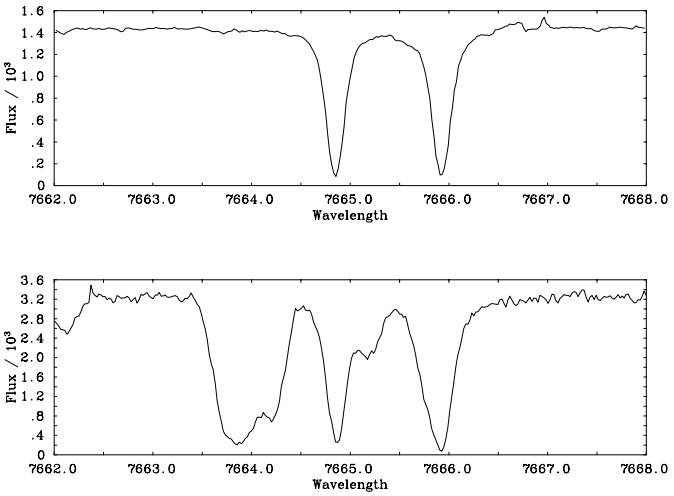

Fig. 4. The 7665 Å K I region in the VLT spectrum of Star 6 (lower panel) compared to a pure telluric spectrum (top panel – see text). Both spectra are at telluric rest. The CS K I component is unaffected by telluric contamination.

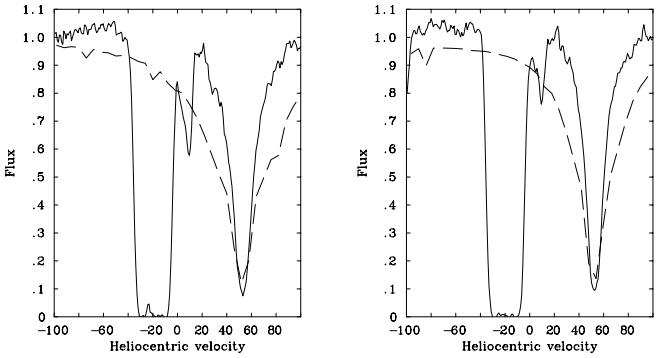

Fig. 5. Na I profiles in the Star 6 VLT spectrum, together with spectral syntheses (dashed lines). The left panel shows Na D1, the right Na D2. The spectra are in velocity space, and the model spectra have been shifted to the photospheric radial velocity.

DIB at 6284 Å is shown, together with a Kurucz synthesis (upper panel) and the pure telluric spectrum of G64-12. A feature can be seen at 6283.80 Å, indicated by a vertical line at this wavelength. This wavelength is very close to the 6283.86 Å central wavelength of the 6284 DIB, derived from ISM studies (Herbig 1995). While this feature is unaffected by telluric lines, the situation is complicated by the Kurucz synthesis prediction of a line coinciding with the possible DIB. The line is Fe I λ6283.729. While the synthesis clearly greatly overestimates the strength of this line, presumably owing to uncertainty in the log gf value, an atomic contribution to the DIB profile cannot be ruled out.

The DIB is observed independently in all 4 spectra of this wavelength region, hence an instrumental origin is ruled out. Its equivalent width is 27 mÅ. Using the 6283.86 Å value as a rest wavelength, a heliocentric velocity of -2.9 km s^{-1} is derived, which is far from the heliocentric velocity of IRC +10° 216. Using the well known correlation of DIB strength to E_{B-V}, it is possible to estimate the reddening from the DIB strength, assuming an origin in the ISM, which seems likely. For HD 183143 (E_{B-V} = 1.28), W_λ for this DIB is 1945 mÅ (Herbig 1995) while for the star μ Sgr (E_{B-V} = 0.25), a well characterised ISM line of sight, W_λ is 167 mÅ (unpublished results of the author). Simple scaling yields E_{B-V} = 0.018 and 0.04 respectively, values that are close to that suggested by the H I maps and galaxy counts of Burnstein & Heiles (1982) for this region.

This argument reinforces the suggestion that the λ6284 feature arises in the ISM, not the IRC +10° 216 CSE. Moreover, its heliocentric velocity is near that of the bluer of the two components seen in Na D in the spectra of ν Leo (see Fig. 6), that are likely to be interstellar. It is probable

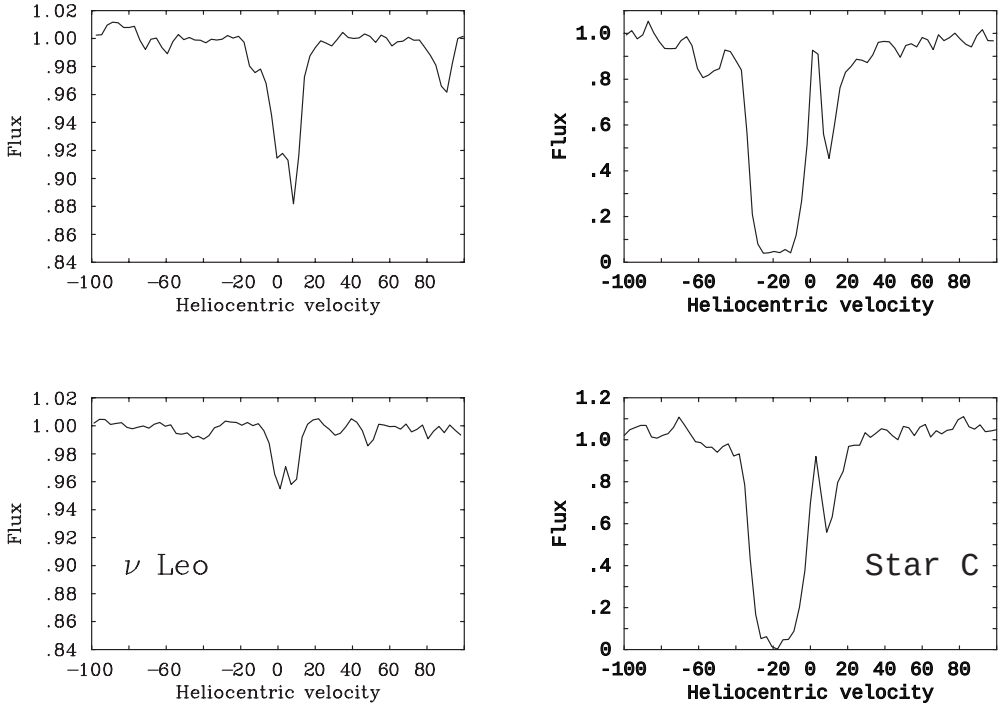

Fig. 6. Na I profiles in the WHT spectra of ν Leo (left panel) and Star C (right panel). D1 is above, D2 below. Note the similarity of the Star C profiles to those in Star 6, and the weakness of the profiles in ν Leo. Note the ordinate scales.

that these Na D components and the λ6284 DIB observed towards Star 6 arise in the same diffuse cloud, which is far closer than Star 6 and even closer than IRC +10° 216, the distance of ν Leo being only 55 pc.

The other strong DIB searched for is λ6614 (see Fig. 8). This wavelength region is free of photospheric and telluric lines. No DIB is observed. An upper limit to the equivalent width of this DIB can be obtained. We assume a width (*FWHM*) of about 0.35 Å, as is shown by the high resolution profiles through clouds with especially narrow Na I lines given by Walker et al. (2000). Then, by applying the method of Cowie & Songaila (1986; their Eq. (3.12)), with $R = 50\,000$ and $S/N = 58$, we find a 3σ upper limit of 16 mÅ. By scaling the case of HD 183143 given by Herbig (1995), this $W(3\sigma)$ corresponds to $A_{\rm v} = 0.18$ mag or $N_{\rm H} = 3.8 \times 10^{20}$ cm^{-2}. Consequently, our 3σ upper limit on the strength of a diffuse circumstellar band at λ6614 is about 5 times smaller than what would be expected from the circumstellar medium, if it obeyed the interstellar relation between $N_{\rm H}$ and the DIB strengths.

We have also examined the regions of the DIBs at 6196, 6203, 6270, 6379, 6993, and 7224 Å. Blends with photospheric lines occur for λ6196, λ6379 and λ7224, but the other three regions are clear, and no diffuse feature is seen with upper limits comparable but not better than the one derived above for λ6614. DIBs have also been sought in the WHT/UES spectrum of Star C. The strongest DIBs in the highest signal-to-noise ratio spectral regions are λ6284 ($S/N \sim 35$) and λ5780 ($S/N \sim 50$). No DIBs are observed.

6. Discussion

The first main result emerging from this work to date is the discovery of two suitable optical targets located behind and seen through the CSE of IRC +10° 216. Star 6 is of special interest, with its offset of 37″, because the CS column density is relatively high, meaning that a new method is now established to study the cold, external, but still molecular layers of this carbon-rich envelope.

The large equivalent widths of the K I lines are important (∼500 mÅ) and are even larger than those found for very reddened OB stars, like Cyg OB2 #9 with $E_{B-V} = 2.25$ (Chaffee & White 1982). We note that the lines appear to be composed of at least three velocity components attributable to sheets of gas, probably incomplete shells, consistent with the results of optical imaging (Mauron & Huggins 1999). A better spectral resolution than used here, (∼6 km s^{-1}), would possibly help to resolve these components and study them separately. Here, we shall adopt a simple approach and consider the observed K I lines as due to a single broad component. One derives from the doublet data a K I column density $N_{\rm KI} \sim 3.0 \times 10^{12}$ cm^{-2}, and a λ7699 line opacity of order unity if a velocity width of the order of the wind expansion speed, i.e. about 10 km s^{-1}, is assumed. This $N_{\rm KI}$ can be readily compared to the expected column density of potassium (i.e. all K nuclei) by using the model envelope parameters of Sect. 2 and a cosmic abundance of K of 1.3×10^{-7} (K is not nucleosynthetized in AGB stars). One finds $N_{\rm K} = 2.4 \times 10^{14}$ cm^{-2}, so that, *on average* along the line of sight in the circumstellar envelope, only about

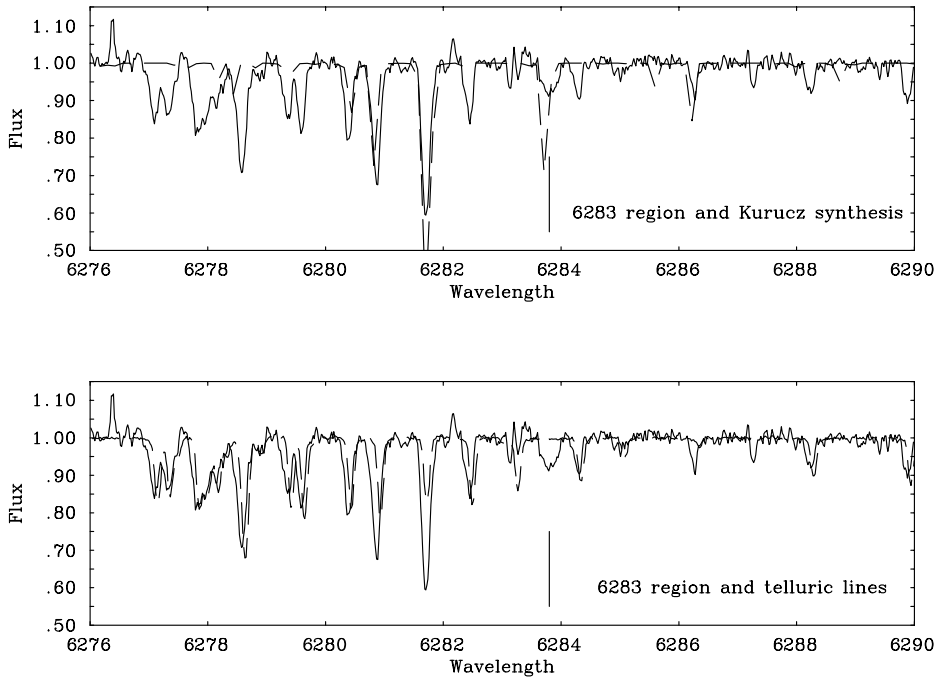

Fig. 7. The region of the 6283 DIB in the Star 6 spectrum. The possible DIB feature is indicated by the vertical line. All spectra are at the heliocentric velocity. The observational data (solid line) is compared to a Kurucz synthesis (top panel) and a pure telluric spectrum (bottom panel).

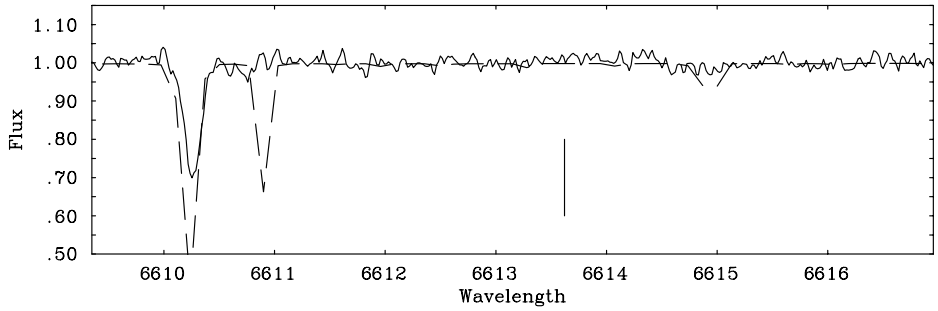

Fig. 8. The region of the 6614 DIB in the Star 6 spectrum. The rest wavelength of the DIB feature is indicated by the vertical line. All spectra are at the heliocentric velocity. The observational data (solid line) is compared to a Kurucz synthesis (dashed line).

1% of K nuclei are in the K I form. For comparison, in the diffuse interstellar medium and for a similar H column density, i.e. for $A_{\rm v} = 0.9$, one usually finds $N_{\rm KI}$ around $4.5 \times 10^{11}\,{\rm cm}^{-2}$, within a factor of 2. This is obtained by scaling the data of the ten stars of the catalogue of Chaffee & White (1982) having E_{B-V} between 0.25 and 0.35, excluding the case of ζ Oph for which one finds 2×10^{12} cm^{-2}. Therefore, our data suggest that on average towards Star 6, the CSE has a $N_{\rm KI} \sim 7$ times larger than that in the common diffuse ISM, for the same $N_{\rm H}$.

A possible explanation for the low KI/K ratio of 1% in the CSE is that the large majority (∼99%) of K atoms are in the ionized K II form, due to photoionization by galactic ultraviolet ($\lambda \leq 2860$ Å) photons penetrating the probed outer layers. It is also possible that some K could reside in molecules (e.g. KCN, KCl), or in dust grains. Similar to KCN, the NaCN molecule has indeed been detected in IRC +10° 216 by Turner et al. (1994). However, there is no clear indication as to the radial extent of the alkali metal-bearing molecules, i.e. whether they still exist (against photodissociation) at the impact parameter of Star 6. In the case of NaCN, there is a large uncertainty, by a factor of 200, on its abundance, but if it forms in the outer envelope, up to 7% of Na can be in NaCN, according to Turner et al. (1994). Little information exists on depletion of K and Na in carbonaceous grains. At present, it is not possible to perform a detailed quantitative budget of these alkali metals and study their evolution along the gas flow. However, this situation may improve in the future with more sensitive molecular maps to be obtained with ALMA, and supplementary optical spectra of Na, K and other atoms towards other background targets.

The second main result concerns DIBs, and especially the question of whether DIB carriers can be found in circumstellar envelopes of evolved stars. Because it is currently favoured that DIBs could arise in large

organic molecules, such as carbon chains, PAHs, C_{60} and related compounds (e.g. cations), one might speculate that diffuse bands would be readily detected throughout the carbon rich envelope of IRC +10° 216. This is not the case. Our spectra show no detectable diffuse band in the envelope of IRC +10° 216. This is in agreement with the findings of Le Bertre & Lequeux (1993), at least for some of the carbon-rich objects they examined. For example, according to these authors, the dusty absorbing circumstellar material of NGC 7027, BD+30° 3639, Hen 1044, CPD-56° 8032, IRAS 21282+5050, HR 4049 and HD 213985 (which are either planetary or proto-planetary nebulae) are *depleted* in DIB carriers relatively to the ISM. However, as noted in Sect. 1, there are two carbon-rich objects, AC Her and especially CS 776, that might have diffuse *circumstellar* bands, according to the same authors.

The case of CS 776 is interesting in our context because it is the only genuine AGB outflow with which we can compare our findings. Le Bertre & Lequeux (1993) found that in the line of sight to the A–type companion of the carbon star, which they argue suffers a *circumstellar* absorption $E_{B-V} = 0.53$, the λ5797 DIB is abnormally weak, compared to λ5780, giving support to the principle of dividing DIBs in families. The strengths of the other DIBs ($\lambda\lambda$4430, 5780, 6284) are in reasonable agreement with ISM-like expectations, with λ5780 being, however, twice as intense. In the context of the present work on IRC +10° 216, we would note that the critical question for CS 776 is whether the reddening is indeed *circumstellar* and not interstellar (see also the comments by Herbig 1995). According to Le Bertre (1990), CS 776 has the following properties: distance 1.3 kpc, mass loss rate of the carbon star $\dot{M}_{\rm H} = 5 \times 10^{-7}\ M_\odot\ {\rm yr}^{-1}$, and $v_{\rm outflow} = 25\,{\rm km\,s}^{-1}$. For its companion at an offset of 1.8″, these characteristics imply a line of sight (tangential) $N_{\rm H} = 5.4 \times 10^{19}\,{\rm cm}^{-2}$, which would correspond in the ISM to $E_{B-V} = 0.0083$. This is much lower than the above $E_{B-V} = 0.53$ attributed to the circumstellar matter by Le Bertre (1990). This $N_{\rm H}$ column density is also much lower than that toward Star 6, for which no DIBs are observed. So, in order to maintain the conclusion of the circumstellar origin (for DIBs and reddening), one has to assume that CS 776 had a much larger mass loss rate in the past (450 yr ago), of the order of $\sim 3 \times 10^{-5}\ M_\odot\ {\rm yr}^{-1}$. Although mass loss from AGB stars is known to undergo time variability, its seems to us that this assumption is less probable than simply envisaging an interstellar origin for the DIBs and the observed reddening. We also note that CS 776 has no mid-infrared excess (with flux densities peaking at 25 or 60 μm), as seen for many post-AGB objects and also a few carbon stars with similar ancient detached envelopes: its IRAS fluxes are 90, 29, 5 and < 15 Jy at 12, 25, 60 and 100 μm, respectively, and are typical of a normal carbon star without a detached shell. Certainly, it would be useful to re-investigate the interstellar reddening in the field of CS 776, and examine again the presence or absence of atomic lines, and DIBs, attributable uniquely to the CS 776 envelope.

It is of interest also to examine our results in the context of other compact objects toward which diffuse circumstellar band carriers have been sought, or indeed observed. For example, it was suggested by our referee to examine a possible H-deficiency in IRC + 10° 216, because another very clear case of DIB absence is that of the circumstellar disk of HR 4049, which might be H-deficient (Waters et al. 1989). Although it is true that there is no *direct* measurement of the abundance of H_2 in IRC +10° 216 (i.e. a measurement of the H_2 loss rate), there are several reasons supporting the case that IRC +10° 216 is not particularly H-poor. The models fitting many molecular observations generally adopt a ratio C/H_2 of $\sim 10^{-3}$, and collisions with H_2 are the main source of excitation of the molecules (e.g. Groenewegen et al. 1998). A large abundance of hydrogen is also indicated by: a) abundant H-bearing molecules such as C_2H_2 or HCN; b) the presence of HCO^+, formed from H_3^+, itself a consequence of cosmic ray induced ionization of H_2 (Glassgold 1996), and c) detection of cold H I at 21 cm (Le Bertre & Gérard 2001).

The absence of diffuse band carriers seen in absorption in the cool carbon-rich layers of IRC +10° 216, and in a number of C-rich planetary nebulae (even those showing UIR features, such as NGC 7027) also suggests comparison with the Red Rectangle. For this object, Schmidt & Witt (1991) have shown that the strong optical emission features attributed to a subset of diffuse band carriers appear only at the bicone interfaces, where carbon-rich material is presumably being eroded by a bipolar plasma flow, and/or by the ultraviolet radiation from the central star. From a study of the spatial distribution and spectral structure of the 3.3 μm UIR feature, Kerr et al. (1999) suggested that through this erosion the grains might produce even completely dehydrogenated DIB-emitting molecules, perhaps monocyclic carbon ring molecules (see also Kerr et al. 1996). If this scenario were correct, the absence of DIBs in the outer layers of IRC + 10° 216 could be understood as arising from the fact that its circumstellar material has not been *processed* at all in a similar way during its formation and ejection history. The effect of the external UV interstellar radiation field on the probed layers of IRC + 10° 216 is probably insufficient to dehydrogenate the dust and fabricate DIB carriers, given the low field intensity, compared to the strong UV irradiation expected from the hot central star of the Red Rectangle. Moreover, the circumstellar dust in IRC + 10° 216 is exposed to UV for only a short time, compared to the ISM. Finally, the average circumstellar density in the line of sight to Star 6, of order 2000 $H_2/{\rm cm}^3$, may also be too large to permit these carriers (if any) to exist freely, as they do in the diffuse low-density ISM and the bipolar cavity of the Red Rectangle.

In summary, these results concerning the prototypical mass-losing AGB star IRC + 10° 216 reinforce the evidence that the DIB carriers are absent, or of very low abundance, in the cool winds of such carbon stars. Furthermore, it is quite plausible that some important processing, perhaps strong UV irradiation, not present in

the observed layers of IRC +10° 216, is needed to fabricate DIB carriers from carbon-rich grain or molecule precursors. The recent observations of possible circumstellar diffuse band carriers in relatively UV-poor F and G–type post-AGB supergiants, as outlined in Sect. 1, will be, if confirmed, a key route for resolving the DIB mystery.

7. Conclusions

1. A unique attempt to probe the circumstellar envelope of IRC +10° 216, using optical absorption spectroscopy towards background stars lying beyond the envelope, has been performed.
2. Analysis using Kurucz model atmospheres and spectral synthesis techniques has been performed for the most favourable target Star 6, located at 37″ from IRC +10° 216. The analysis confirms that this target is much more distant than the carbon star envelope; the target is found to be a somewhat metal-poor G-dwarf with $T_{\rm eff} = 5650$ K.
3. The circumstellar hydrogen column density towards this target is expected to be $\sim 1.8 \times 10^{21}$ cm^{-2}, which would correspond to $A_{\rm v} = 0.9$ mag in the diffuse interstellar medium, and hence the expectation of strong DIBs. Extinction maps of the field suggest also that there is little contamination of the line-of-sight by foreground or background interstellar matter, with $A_{\rm v}$ (ISM) $\lesssim 0.1$ mag.
4. The IRC+10°216 CSE is definitely detected in K I and most probably in Na I also. Circumstellar Na I is very probably also detected towards a second target located at 153″ from IRC +10° 216.
5. Diffuse band absorptions arising in the circumstellar envelope are not observed. The strong DIB, λ6284, is detected, but its origin is interstellar. The weakness of the DIB is commensurate with the known low reddening towards this region, and its observed velocity also negates a circumstellar origin.
6. Overall, the data suggest that no DIB carrier exists in the envelope of IRC +10° 216 with the abundances relative to hydrogen typical of the diffuse ISM.

Acknowledgements. We are grateful to the Leverhulme Trust for an award and for the support of one of us (TRK) and NM thanks the French Programme National of CNRS *Physico-chimie du Milieu Interstellaire*. We thank the WHT service observing support staff, and acknowledge with thanks use of CDS (Centre de Données de Strasbourg) and the ESO/ECF Centre for archive material. Lastly, we are grateful for the comments of an anonymous referee.

Appendix A: Details on the derivation of photospheric parameters for the main target Star 6

In this Appendix, we describe the steps undertaken to derive the photospheric parameters for Star 6 from its UVES spectrum. Initially, the equivalent widths of 228 lines of Fe I were measured throughout a wavelength range of 4786−6752 Å, corresponding to the highest signal-to-noise ratio spectral segments which were relatively unaffected by telluric lines. These lines yielded a heliocentric radial velocity for Star 6 of $+52.4 \pm 0.6$ km s^{-1}.

Table A.1. Elemental abundances for the Star 6 photosphere, relative to the solar abundance. Adopted solar values are given in the last column. N is the number of lines used for each species. For clarity, elements are divided into α elements, Fe group elements, and others. Sources for gf-values are indicated.

Element	[X/H]/dex	N	[X/H]$_\odot$ [a]
Ti [b]	−0.25	50	4.99
Si [c]	−0.12	12	7.55
Mg [d]	−0.19	4	7.58
Ca [e]	−0.38	31	6.36
O [f]	−0.01	4	8.93
Fe [g]	−0.39	214	7.55
Co [h]	−0.17	21	4.92
Cr [i]	−0.47	45	5.68
Ni [c]	−0.39	21	6.25
Na [c]	−0.24	3	6.32
C [j]	−0.22	7	8.57

[a] Anders & Grevesse (1989), [b] Grevesse et al. (1989), [c] gf-values derived from solar equivalent widths using abundances of (a), [d] Thévenin (1989), Thévenin (1990), [e] Smith & Raggett (1981), [f] Biémont et al. (1991b), [g] see Refs. in text, [h] Cardon et al. (1982), [i] Blackwell et al. (1984), Blackwell et al. (1986b), [j] Biémont et al. (1993).

The equivalent widths of 88 relatively weak (≤60 mÅ) lines were used to obtain a first estimate of $T_{\rm eff}$ and simultaneously, metallicity. By minimising the gradient of a plot of log [Fe] vs. the excitation potential χ (using the log gf values of O'Brian et al. 1991; Bard et al. 1991; Blackwell et al. 1986a and references therein), values of $T_{\rm eff} = 5650 \pm 50$ K and [Fe/H] = −0.36 dex relative to solar, were obtained.

Using these values of $T_{\rm eff}$ and [Fe/H], the equivalent widths of 214 Fe I lines (including the 88 above) were used to derive the microturbulent velocity $V_{\rm turb}$, by minimising the gradient of a plot of log [Fe] vs. log (W_λ/λ). A best value of 1.3 km s^{-1} was obtained, together with a second metallicity estimate of [Fe/H] = −0.41 dex, relative to solar.

The third step was to use the equivalent widths of Fe II lines, and the log gf values of Biémont et al. (1991a), to derive log g by varying log g until [Fe/H] converged on the value yielded by the Fe I lines. Using 28 lines, a value of log $g = 4.3 \pm 0.1$ was found, with [Fe/H] = −0.39 dex.

With metallicity values converging on [Fe/H] = −0.4 dex relative to solar, a final model of $T_{\rm eff} = 5650$ K, log g = 4.3 (cgs), $V_{\rm turb}$ = 1.3 km s^{-1} and [Fe/H] = −0.4 dex has been adopted. Using this model, abundances for other elements were derived and are given in Table A.1. With the exception of oxygen, all derived abundances lie in the range −0.1−0.5 dex relative to solar, with the α

elements perhaps being less underabundant than the Fe group elements. The oxygen abundance is obtained from only four lines, three of which are the O I triplet at 7772, 7774 and 7775 Å, which are known to yield higher abundances than other O I lines (Nissen & Edvardsson 1992).

A similar analysis was performed to derive the photospheric parameters for Star C, to obtain a spectroscopic distance estimate. Owing to the poorer quality of the spectrum, no individual elemental abundances were derived. From 82 Fe I lines, $T_{\rm eff}$ in the range 6200−6250 K was derived, with $V_{\rm turb} = 2.1{-}2.2$ km s^{-1} obtained using a further 78 stronger lines. The surface gravity was not well constrained (using 21 Fe II lines) and is certainly >4.5 and possibly as high as 5.0. A metallicity [Fe/H] of -0.4 ± 0.1 dex (relative to solar) has been adopted.

References

Allen, C. W. 1973, Astrophysical Quantitie, 3rd ed. (Athlone Press)
Anders, E., & Grevesse, N. 1989, Geo. Co. A., 53, 197
Axer, M., Fuhrmann, K., & Gehren, T. 1994, A&A, 291, 895
Bakker, E. J., van Dishoeck, E. F., Waters, L. B. F. M., & Schoenmaker, T. 1997, A&A, 323, 469
Bard, A., Kock, A., & Kock, M. 1991, A&A, 248, 315
Beintema, D. A., van den Ancker, M. E., Molster, F. J., et al. 1996, A&A, 315, L369
Biémont, E., Baudoux, M., Kurucz, R. L., Ansbacher, W., & Pinnington, E. H. 1991a, A&A, 249, 539
Biémont, E., Hibbert, A., Godefroid, M., Vaeck, N., & Fawcett, B. C. 1991b, ApJ, 375, 818
Biémont, E., Hibbert, A., Godefroid, M., & Vaeck, N. 1993, ApJ, 412, 431
Blackwell, D. E., Menon, S. L. R., & Petford, A. D. 1984, MNRAS, 207, 533
Blackwell, D. E., Booth, A. J., Haddock, D. J., & Petford, A. D. 1986a, MNRAS, 220, 549
Blackwell, D. E., Booth, A. J., Menon, S. L. R., & Petford, A. D. 1986b, MNRAS, 220, 303
Bohlin, R. C., Savage, B. D., & Drake, J. F. 1978, ApJ, 224, 132
Burnstein, D., & Heiles, C. 1982, AJ, 87, 1165
Cami, J., Sonnentrucker, P., Ehrenfreud, P., & Foing, B. H. 1997, A&A, 326, 822
Cardon, B. L., Smith, P. L., Scalo, J. M., Testerman, L., & Whaling, W. 1982, ApJ, 260, 395
Chaffee, F. H. Jr., & White, E. E. 1982, ApJS, 50, 169
Cowie, L. L., & Songaila, A. 1986, ARA&A, 24, 499
Douglas, A. E. 1977, Nature, 269, 130
Foing, B. H., & Ehrenfreud, P. 1997, A&A, 317, L59
Galazutdinov, G. A., Krelowski, J., Moutou, C., & Musaev, F. A. 1998, MNRAS, 295, 437
Galazutdinov, G. A., Musaev, F. A., Krelowski, J., & Walker, G. A. H. 2000, PASP, 112, 648
Glassgold, A. E. 1996, ARA&A, 34, 241
Grevesse, N., Blackwell, D. E., & Petford, A. D. 1989, A&A, 208, 157
Groenewegen, M. A. T., van der Veen, W. E. C. J., & Matthews, H. E. 1998, A&A, 338, 491
Herbig, G. H. 1995, ARA&A, 33, 19
Howarth, I. D., Murray, J., Mills, D., & Berry, D. S. 1998, Starlink User Note 50.21
Huggins, P. J. 1995, Ap&SS, 224, 281
Kerr, T. H., Hibbins, R. E., Miles, J. R., et al. 1996, MNRAS, 283, L105
Kerr, T. H., Hurst, M. E., Miles, J. R., & Sarre, P. J. 1999, MNRAS, 303, 446
Klochkova, V. G., Szczerba, R., Panchuk, V. E., & Volk, K. 1999, A&A, 354, 905
Klochkova, V. G., Szczerba, R., & Panchuk, V. E. 2000, Astr. Lett., 26, 88
Klochkova, V. G., Panchuk, V. E., & Szczerba, R. 2000, in Post-AGB objects as a Phase of Stellar Evolution, ed. R. Szczerba, & S. K. Gorny (Kluwer Academic Publishers)
Kroto, H. W., & Jura, M. 1992, A&A, 263, 209
Kurucz, R. L. 1991, in Precision Photometry: Astrophysics of the Galaxy, ed. A. G. Philip, A. R. Upgren, & P. L. Janes (L. Davis Press, Schenectady), 27
Lang, K. R. 1991, Astrophysical Data: Stars and Planets (Springer-Verlag)
Le Bertre, T. 1990, A&A, 236, 472
Le Bertre, T., & Lequeux, J. 1992, A&A, 255, 288
Le Bertre, T., & Lequeux, J. 1993, A&A, 274, 909
Le Bertre, T., & Gérard, E. 2001, A&A, 378, L29
Léger, A., d'Hendecourt, L., & Bocarra, N. (ed.) 1987, Polycyclic Hydrocarbons and Astrophysics (Dordrecht: Reidel)
Mauron, N., et al. 2002, in preparation
Mauron, N., & Huggins, P. J. 1999, A&A, 349, 203
Miles, J. R., & Sarre, P. J. 1993, J. Chem. Soc. Farad. Trans., 89, 2269
Molster, F. J., van den Ancker, M. E., Tielens, A. G. G. M., et al. 1996, A&A, 315, L373
Nissen, P. E., & Edvardsson, B. 1992, A&A, 261, 255
O'Brian, T. R., Wickliffe, M. E., Lawler, J. E., Whaling, W., & Brault, J. W. 1991, J. Opt. Soc. Amer. B, 88, 1185
Omont, A. 1991, in Chemistry of Space, ed. J. M. Greenberg, & V. Pironello, 171
Rao, N. K., & Lambert, D. L. 1993, MNRAS, 263, L27
Salama, F., Bakes, E. L. O., Allamendola, L. J., & Tielens, A. G. G. M. 1996, ApJ, 458, 621
Sarre, P. J., Miles, J. R., & Scarrott, S. M. 1995, Science, 269, 674
Schmidt, G. D., & Witt, A. 1991, ApJ, 383, 698
Smith, G., & Raggett, D. 1981, J. Phys. B Atom. Mol. Phys., 14, 4015
Snow, T. P., & Wallerstein, G. 1972, PASP, 84, 492
Snow, T .P. 1973, PASP, 85, 590
Sorokin, P. P., & Glownia, J. H. 1996, ApJ, 473, 900
Thaddeus, P., Gottlieb, C. A., Mollaaghababa, R., & Vrtilek, J. M. 1993, J. Chem. Soc. Farad. Trans. 89, 2125
Thévenin, F. 1989, A&AS, 77, 137
Thévenin, F. 1990, A&AS, 82, 179
Turner, B. E., Steimle, T. C., & Meerts, L. 1994, ApJ, L97
Ubachs, W., Hinnen, P. C., & Reinhold, E. 1997, ApJ, 476, L93
Walker, G. A. H., Bohlender, D. A., & Krelowski, J. 2000, ApJ, 530, 362
Waters, L. B. F. M., Lamers, H. J. G. L. M., Snow, T. P., et al. 1989, A&A, 211, 208
Weselak, T., Schmidt, M., & Krelowski, J. 2000, A&AS, 142, 239
Williams, D. A. 1996, Ap&SS, 237, 243
Zacs, L., Schmidt, M. R., & Szczerba, R. 1999, MNRAS, 306, 903